Two-dimensional hydration shells of alkali metal ions at a hydrophobic surface

Sheng Meng, D. V. Chakarov, B. Kasemo, and Shiwu Gao[a)]
Department of Applied Physics, Chalmers University of Technology and Göteborg University, SE-412 96 Göteborg, Sweden

(Received 9 June 2004; accepted 17 September 2004)

We study the hydration shell formation of alkali metal ions at a graphite surface. Two-dimensional shell structures are found in the initial stage of hydration, in contrast to the three-dimensional structures in bulk water and clusters. Comparison of vibrational spectra with experiments identifies the shell structures and the thermally induced transition from the first to the second shell. We also found intriguing competition between hydration and ion–surface interaction, leading to different solvation dynamics between K and Na. Implications of these results in ionic processes at interfaces are elaborated. © *2004 American Institute of Physics.* [DOI: 10.1063/1.1827215]

Ion hydration at surfaces and interfaces is central to many physical,[1,2] chemical, and biological processes.[3] Examples include the physics of coadsorption, the electrical double layers at the electrolyte/electrode interfaces, hydrated ions in corrosion attacks on materials, ion penetration through cell membranes,[4] and hydration shells around proteins and DNA molecules. The local structure and the stability of the water shells determine the ion mobility, chemical reactivity, and the physiological functions. So far, hydration shells have been studied extensively in aqueous solutions and nanometer clusters, where water is known to form three-dimensional (3D) shell structures.[5–9] Ion hydration at surfaces and interfaces is less understood,[10,11] due to the complications introduced by the broken symmetry and the charge transfer involved in the hydration processes. The latter requires an accurate account of the electronic structure of the water–ion–surface systems. Here, we present a study of hydration shell formation of K and Na ions on a hydrophobic surface. We find that the initial ion hydration shells at the surface are two-dimensional (2D), in contrast to the 3D counterparts in clusters and liquid.

Our study is based on *ab initio* molecular dynamics (MD) simulations of a model system, $K(Na)+nH_2O$ ($n=1-10$), on a graphite(0001) surface. Ionization of the alkali atoms by the surface[12,13] lead to an electric double layer, similar to the Helmholtz layer presented in a variety of solid–liquid interfaces. The hydration shells at the surface are found to be 2D with three and four molecules sitting in the first shells of K and Na, respectively. These 2D shells evolve into different 3D structures as the size increases. The K shell approaches a hemisphere with the ion always staying on the surface. In contrast, the Na ions are gradually separated from the surface and are eventually solvated into the water. This difference reflects the competition between the ion–surface and the ion–water interactions. Vibrational spectra for these 2D structures are calculated. Comparison with recent experiments[12,13] identifies the shell structures and the thermally induced transition from the first to the second shell observed in the experiment. The 2D hydration shells and the dynamical competition between the hydration and ion–surface interaction, have general implications to ionic processes at solid–liquid interfaces and in biological systems.

The calculation was performed with the Vienna *ab initio* simulation program VASP,[14] as used in our earlier studies of water at surfaces.[15,16] The supercell consists of one layer of graphite sheet (separated by 17 Å) in a 4×4 unit cell, an adsorbed K (Na) atom, and nH_2O with $n=1-10$. The adsorbed ions and water molecules were put on one side of the slab. This unit cell corresponds to an ion coverage of 1.2×10^{14} atoms/cm^2, comparable to that in the experiment.[12] The much weaker interlayer coupling of graphite [35 meV (Ref. 17)] is neglected. The ionization of alkali metal atoms at the graphite surface lead to strong ionic interactions in the hydration shells and with the surface, which prevail any possible contribution (if any) from the van der Waals (vdW) interaction. A plane wave cutoff of 300 eV and a $3\times3\times1$ *k*-point sampling was used. The shell structures were determined by typically 4–8 ps molecular dynamics (MD) simulations at 85 K. The energetics was extracted by further relaxation. We used Vanderbilt ultrasoft pseudopotentials for electron interaction with an ion nucleus, and the PW91 form of exchange-correlation energy. Extensive comparison between different functionals shows that PW91 (and its derivatives PBE) is promising for describing the hydrogen bonding and bulk water.[18,19] In particular, it has been shown to be most successful for surface systems.[20]

Before studying the hydration process, adsorption of K and Na atoms on graphite(0001) was studied in details. All results including the binding energies, the adsorption heights, and vibrational frequencies compare well with available experimental data. For example, the hollow site [see Fig. 1(a)] is the most stable, with adsorption energies of 1.01 (K) and 0.75 eV (Na), and adsorption heights of 2.70 Å (K) and 2.36 Å (Na) above the surface, as shown in Table I. The experimentally measured adsorption energies are 1.15 eV (K) and

a)Author to whom correspondence should be addressed; electronic mail: tfysg@fy.chalmers.se

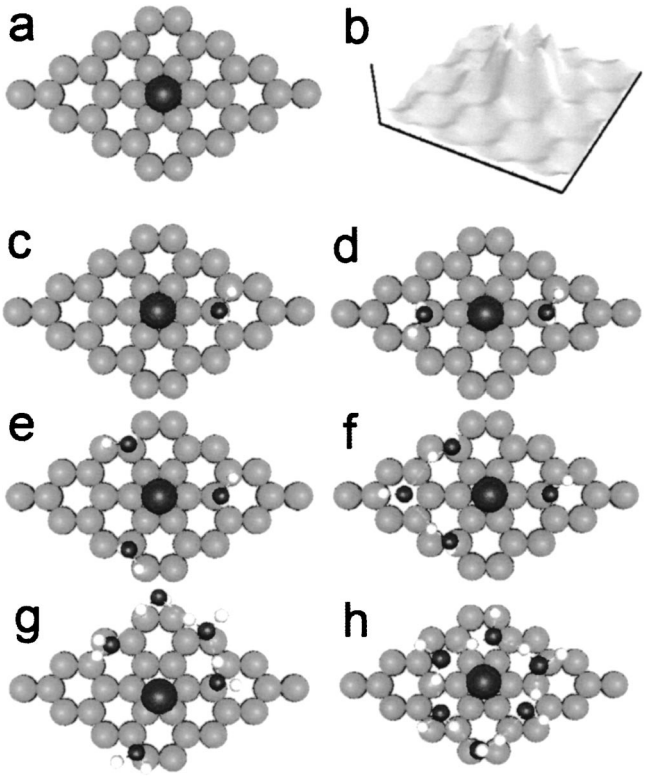

FIG. 1. (a) Adsorption site and (b) electron distribution, at 0.85 Å above the surface, of the ionized K on graphite(0001). (c)–(h) The 2D hydration structures for $K+nH_2O$, $n=1-6$, respectively, on the surface.

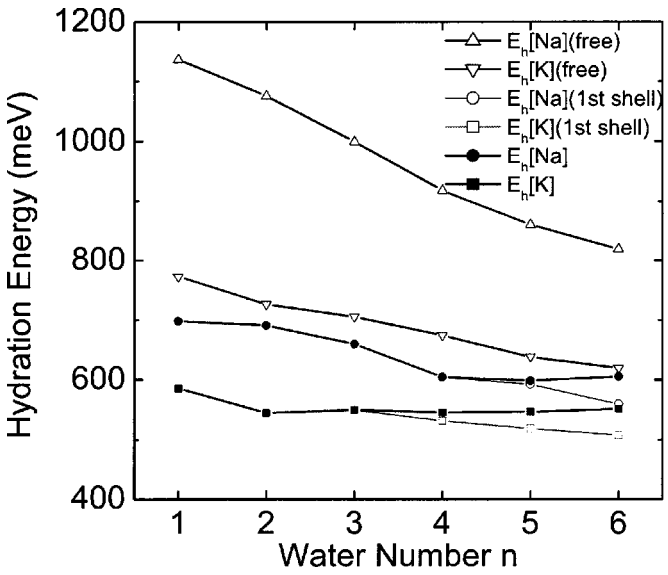

FIG. 2. Hydration energy, $E_h=\{E[\mathrm{K(Na)/C}]+nE[H_2O]-E[\mathrm{K(Na)}+nH_2O/\mathrm{C}]\}/n$, versus the number of water n in the K and Na hydration shells on graphite(0001). Here, E_h measures the average hydration energy per H_2O. The thin lines are for the metastable structures obtained from geometrical optimization by forcing all molecules in the first shell. They transform into the thick lines in MD simulations at 85 K. E_h (free) shows the hydration energies for the free ion–water clusters (see Refs. 21 and 25).

0.77 eV (Na),[13] respectively. The local density of states of the 4*s* (K) and 3*s* (Na) orbitals (not shown here) lies dominantly above the Fermi level. A detailed charge-density analysis indicates that the K ion has $+0.68e$ charge while the Na has $+0.61e$. The ionized electron is distributed mainly in the hybridized $s+p_z$ orbitals of the six neighboring carbon atoms [Fig. 1(b)].

When water molecules are added to K(Na)/graphite, they tend to adsorb around the ionized K(Na) atoms, due to the strong ion–water interaction. We first focus our discussion on the K case, and later compare the Na with the K case. The hydration process of $K+nH_2O$, with $n=1-10$, can be divided into three stages, as detailed below. The structure, the bonding mechanism, and the vibrational spectra are very different at the three stages.

Stage I, $n\leqslant 3$. Formation of the first hydration shell. Water monomer binds to the K ion via primarily the ionic K–O attraction, as shown in Fig. 2, with a binding energy of 0.59 eV. The monomer is adsorbed at a next-nearest-neighbor atop site as shown Fig. 1(c), and can rotate almost freely around the ion, with a barrier of ~10 meV. With additional water ($n=2-3$), the repulsion between O ions tends to keep the molecules away from each other, leading to the linear [$n=2$, Fig. 1(d)], and trigonal [$n=3$, Fig. 1(e)] structures. The K ion accommodates up to three water molecules in the first shell, with all molecules lying in the same plane, as in free clusters.[21,22] One difference here is that the OH bonds are ordered with one OH oriented toward the surface, forming an OH...C hydrogen bond, while the other OH is free. This OH ordering is caused by the electron transfer, which is further enhanced when the first shell forms. The OH...C bond, weak in the gas phase and at the water–graphite interface,[23] should be strengthened by the surface charge transfer.[24]

TABLE I. Adsorption heights (d) and energies (E_{ads}) for K and Na on graphite(0001) surface.

	Hollow		Top	
	d/Å	E_{ads}/eV	d/Å	E_{ads}/eV
K/graphite	2.70	1.01	2.83	0.95
Na/graphite	2.38	0.75	2.62	0.70

Stage II, $4\leqslant n\leqslant 6$. The second hydration shell in 2D. The hydration shells in clusters grow into 3D in this range.[21] On the surface, they continue to be 2D. At $n=4$, the fourth molecule prefers to sit on the surface in the second shell [Fig. 1(f)] rather than forming a tetrahedron or sitting atop the K. The latter configurations are 60–270 meV less stable. This site preference results from the fact that making 2 H-bonds to the first shell ($2\times 0.35=0.7$ eV) is energetically more favorable than forming a fourth K–water bond (at most 0.59 eV as shown in Fig. 2). The enhanced H-bonding to the surface also favors the 3+1 structure. Here, n_1+n_2 denotes the coordination number in the first (n_1) and the second shell (n_2). Besides the energetics, rotational entropy[25] also facilitates the 3+1 structure rather than 4+0, as has been justified from the MD simulation. At $n=5$ and 6, 2D water shells were found to be 3+2 and 3+3, respectively, and remain on the surface, as shown in (g) and (h) of Fig. 1. The $K+6H_2O$ hydration shell is a puckered hexagonal ring, similar to that in ice bilayers on a metal surface.[15,16,26]

Stage III, $n\geqslant 7$. A 3D shell structure starts to emerge. As

TABLE II. The most stable hydration shells, found from MD simulations, for K and Na coadsorbed with nH_2O on graphite, with $n=1-10$. Here $E_h=\{E[\mathrm{K(Na)/C}]+nE[H_2O]-E[\mathrm{K(Na)}+nH_2O/\mathrm{C}]\}/n$ (in eV) is the average hydration energy per H_2O molecule, and n_1+n_2 specifies the number of water molecules in the first (n_1) and second (n_2) shell at the given n.

n	1	2	3	4	5	6	7	8	9	10
E_h[K]	0.59	0.54	0.55	0.55	0.55	0.55	0.57	0.58	0.59	0.59
n_1+n_2	1+0	2+0	3+0	3+1	3+2	3+3	3+4	3+5	3+6	3+7
E_h[Na]	0.70	0.69	0.66	0.60	0.60	0.61	0.60	0.62	0.58	0.61
n_1+n_2	1+0	2+0	3+0	4+0	4+1	4+2, 3+3	4+3	4+4	4+5	4+6

$n\rightarrow 10$, a hemisphere-like structure appears. They can be viewed as a half-shell of the hydrated ions formed in liquid water.[21] This result is reasonable, because the effect of the surface gradually diminishes as the shell grows. Table II summarizes the hydration shell structure and the hydration energy from the calculations. The hydration energies for $n=1-6$ are plotted in Fig. 2, in comparison with those for the free ions. The hydration energies at the surface are generally smaller compared to the free ions, due to the partial ionization of the metal atoms at the surface. Charge density analysis indicates a strong size-dependent electron polarization and depolarization (not shown here) involved in the hydration process. Such a dynamical charge transfer, which is general to all ionic processes at the surfaces, can only be handled to sufficient accuracy in *ab initio* simulations.

We would like to point out, at this point, that the fundamental interaction involved in the hydration at the graphite surface is primarily the ionic interaction rather than the weak van der Waals forces, which are essential in the water–(bare)graphite interaction (~160 meV for monomer/graphite[27]) as well as interlayer coupling [35 meV (Ref. 17)] of bulk graphite. This is due to the ionization of the alkali metal atoms by the surface, leading to a positively charged ion and a negatively charged surface (the so-called electric

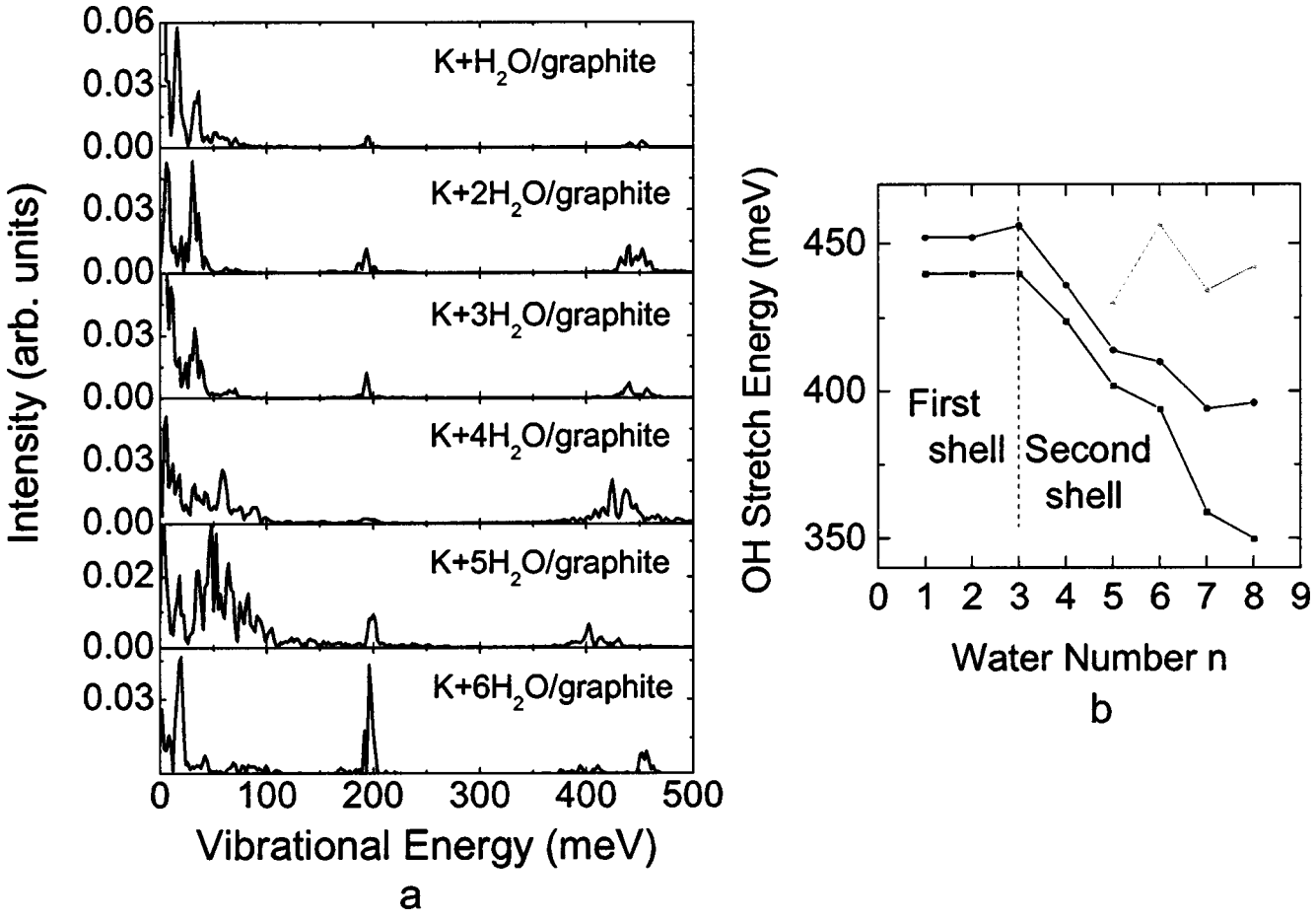

FIG. 3. (a) Vibration spectra for $K+nH_2O$, $n=1-6$, on graphite. (b) The variation of the OH stretch modes with n. These modes are broadened into bands and redshifted at $n\geqslant 4$, where the two lower lines sketch the energy range of the OH bands.

TABLE III. Calculated and experimental vibrational energies (in units of meV) for the K hydration shells on graphite(0001). Experimental data are taken from Ref. 12.

	Translations and librations						δ_{HOH}	$\nu_{O-H}(S)$	$\nu_{O-H}(AS)$
First shell	16	32		51	71		194	440	452
Expt. (85 K)		37		51	79		203	438	457
Second shell	18	34	42	51	85	101	198	394,402,412,424,436	456
Expt. (120 K)			41	51	85	105	203	439	

double layer). The latter in turn results in strong ionic interactions between the ion and the surface (0.75–1.01 eV), and between the water molecules and the ion (0.6–0.7 eV). Furthermore, the DFT/VASP is quite successful in reproducing the work function change and thus the charge transfer between water and surfaces, and between alkali metals and the graphite. As a final remark, the dipole–dipole interaction between supercells is small. For example, the dipole interaction between adjacent adsorbate-graphite layers is 21 and 77 meV for $K+5H_2O$/graphite and $Na+9H_2O$/graphite, respectively. Including the dipole correction with the Neugebauer–Scheffler method,[28] the O–K and K–surface bond length are found to vary by less than 2%. Moreover, the *intercellular* dipole–dipole interaction does not contribute to the hydration energy, which is *intracellular*.

To recognize these structures, vibrational spectra for the $K+nH_2O$/graphite ($n=1-6$) are given in Fig. 3(a). These spectra contain the low-energy librational modes to the left, the HOH scissoring mode at ~200 meV, and the OH stretch modes to the right. The vibrational spectra look similar for $n=1-3$, because the inter-water interaction is small in the first shell. The OH stretch modes are 440 meV (symmetric) and 452 meV (asymmetric), redshifted from the values 454 and 466 meV,[29] for the free H_2O. As $n\geqslant 4$, more modes show up in the 80–105 meV region, while the OH modes are further redshifted and broadened. The evolution of the OH modes is sketched in Fig. 3(b). Characteristic OH modes can be found at 424 and 436 meV for $K+4H_2O$; 402, 414, and 430 meV for $K+5H_2O$; and 394, 410, and 456 meV for $K+6H_2O$. The two lower lines in Fig. 3(b) at $n\geqslant 4$ sketch the range of the OH bands. A transition at $n=4$ is clearly seen as a signature for the second-shell formation. In addition, a high-energy mode at 450 meV, corresponding to the free OH stretch of the peripheral molecules, is also discernible. The redshift of the OH stretch and the appearance of low energy modes are characteristic for the H-bonding in the second shell.

While the predicted vibrational spectra await for experimental justification in future, it is interesting to compare Fig. 3 with the electron energy loss spectroscopy[12] for coadsorbed K and water on the graphite (Table III). The experiment was carried out for $K+H_2O$/graphite at 85 and 120 K, and at similar coverages of K and water. The translational and rotational modes at 32, 51, and 71 meV for $n=1-3$ compare well with the experimental data at 37, 51, and 79 meV at 85 K, when water is deposited on the potassium covered surface. It suggests that the initial coadsorption of water and K only forms the first hydration shell, although we can not tell n among $n=1-3$. In contrast, the rotational/librational modes in the 40–110 meV range agree well with those modes observed at 120 K, when the sample is heated up.[12] Our results then suggest the formation of the second shell, which is likely activated by water diffusion along the surface. A detailed comparison suggests that the 120 K spectrum matches well with those at $n=4-5$. Our best guess,

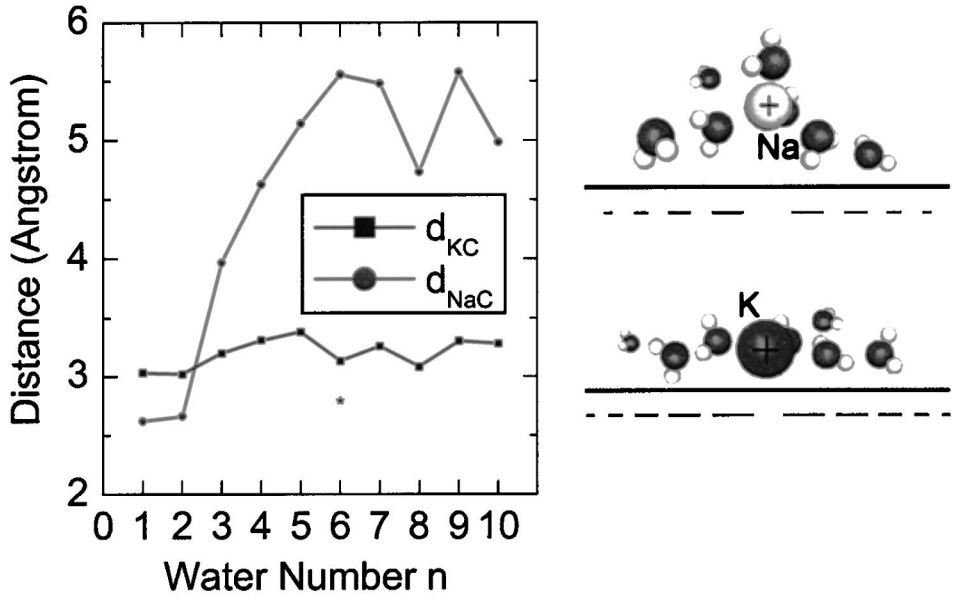

FIG. 4. The ion–surface distance as a function of *n*. These distances were averaged over 4–8 ps MD trajectories for the simulated systems. The star at $Na+6H_2O$ corresponds to a 3+3 structure, which is equally stable as the puckered 4+2 structure.

after comparing all modes, is $n=5$, for that experiment.

Let us now study a different yet general aspect of ionic hydration at surfaces; namely, the competition between hydration and the ion–surface interaction. Two such fundamental interactions are responsible for all static properties and the dynamical processes involving an aqua-ion system at the interfaces. For this purpose, we compare the Na/graphite with the K/graphite. It is known that: (i) Na has a larger ionization energy, and is less ionized on graphite; (ii) The ionic radius of Na (1.13 Å) is smaller than that of K (1.51 Å),[30] due to its more tightly bound $2p$ orbitals. This difference implies a stronger hydration force in the Na/graphite.

Similar to the K case, the shell structure for Na $+nH_2O$/graphite can also be divided into three types: (i) the first shells at $n=1-4$, (ii) the second 2D shells at $n=5-6$, and (iii) the bulk water limit, at larger n. The hydration energies are also shown in Fig. 2. A much stronger hydration energy is found for all n studied (0.70 eV for $n=1$), suggesting a much stable shell structure. The hydration energy decreases as n increases,[31] due to the gradual transition from the strong ion–water interaction to the inter-water H-bonding. Associated with this transition, the energy difference between K and Na becomes smaller at large n. It is worth mentioning that a more stable structure of Na shell was believed to play a key role in the selectivity of K ion channels,[4] where the energy cost for depriving the hydration shell competes sensitively with the energy gain in entering the ion channels.

What differs most between K and Na is the solvation dynamics shown in Fig. 4 by the ion–surface distance as a function of n. The K ion stays on the surface for all n values studied and does not dissolve. In contrast, the Na–surface distance increases gradually as n increases. At $n=10$, the Na ion is almost solvated into water. This difference results from the competition between hydration and ion–surface interaction. The hydration force wins in the Na case.

Summarizing, we have found 2D hydration shells of K and Na ions at the graphite surface, and the intriguing competition between hydration and ion–surface interaction. These results, though obtained on two specific systems, have general implications to other ionic processes at surfaces and interfaces. One can speculate, for example, that ion transport at solid–liquid interfaces may involve dynamical transformations between 2D (when the ion is close to a surface) and 3D water shells (when the ion is away from the surface). The charge transfer associated with the structural transformation implies that it is essential to describe the ionic hydration from the electronic structure of the systems. Finally, the understanding that we gained here at a flat surface is also an important step towards studying ionic processes at more complex surfaces such as curved walls and confined geometries, which may better represent a biological environment and processes, although the effect of the geometric structures and chemical specificity of such surfaces remain to be explored.

This work was supported by the Swedish Research Council (VR) through VR 621-2001-2614 and by NUTEK via grant Dnr 02767.

[1] P. A. Thiel and T. E. Madey, Surf. Sci. Rep. **7**, 211 (1987).
[2] M. A. Henderson, Surf. Sci. Rep. **46**, 1 (2002).
[3] B. Kasemo, Surf. Sci. **500**, 656 (2002).
[4] D. A. Doyle, J. M. Cabral, R. A. Pfuetzner, A. Kuo, J. M. Gulbis, S. L. Cohen, B. T. Chait, and R. MacKinnon, Science **280**, 69 (1998).
[5] M. Y. Kiriukhin and K. D. Collins, Biophys. Chem. **99**, 155 (2002).
[6] M. E. Tuckerman, D. Marx, and M. Parrinello, Nature (London) **417**, 925 (2002).
[7] W. H. Robertson, E. G. Diken, E. A. Price, J.-W. Shin, and M. A. Johnson, Science **299**, 1367 (2003).
[8] M. F. Kropman and H. J. Bakker, Science **291**, 2118 (2001).
[9] A. W. Omta, M. F. Kropman, S. Woutersen, and H. J. Bakker, Science **299**, 1367 (2003).
[10] Y. K. Cheng and P. J. Rossky, Nature (London) **392**, 696 (1998).
[11] S. Baldelli, G. Mailhot, P. N. Ross, and G. A. Somorjai, J. Am. Chem. Soc. **123**, 7697 (2001).
[12] D. V. Chakarov, L. Österlund, and B. Kasemo, Langmuir **11**, 1201 (1995).
[13] L. Österlund, D. V. Chakarov, and B. Kasemo, Surf. Sci. **420**, 174 (1999).
[14] G. Kresse and J. Hafner, Phys. Rev. B **47**, 558 (1993).
[15] S. Meng, L. F. Xu, E. G. Wang, and S. W. Gao, Phys. Rev. Lett. **89**, 176104 (2002).
[16] S. Meng, E. G. Wang, and S. W. Gao, J. Chem. Phys. **119**, 7617 (2003).
[17] L. X. Beredict, N. G. Chopra, M. L. Cohen, A. Zettl, S. G. Louie, and V. H. Crespi, Chem. Phys. Lett. **286**, 490 (1998).
[18] S. Tsuzuki and H. P. Lüthi, J. Chem. Phys. **114**, 3949 (2001).
[19] D. R. Hamann, Phys. Rev. B **55**, R10157 (1997).
[20] For example, the PW91/PBE gives a much smaller mean error (4.9%) to the surface exchange-correlation energy than other commonly used functionals, like the Becke–Lee–Yang–Parr functional, whose mean error is seven times larger (i.e., 34.8%) at surfaces. S. Kurth, J. P. Perdew, and P. Blaha, Int. J. Quantum Chem. **75**, 889 (1999).
[21] O. Borodin, R. L. Bell, Y. Li, D. Bedrov, and G. D. Smith, Chem. Phys. Lett. **336**, 292 (2001).
[22] D. Feller, E. D. Glendening, D. E. Woon, and M. W. Feyereisen, J. Chem. Phys. **103**, 3526 (1995).
[23] D. Feller and K. D. Jordan, J. Phys. Chem. A **104**, 9971 (2000).
[24] S. W. Gao, J. R. Hahn, and W. Ho, J. Chem. Phys. **119**, 6232 (2003).
[25] J. Kim, S. Lee, S. J. Cho, B. J. Mhin, and K. S. Kim, J. Chem. Phys. **102**, 839 (1995).
[26] D. L. Doering and T. E. Madey, Surf. Sci. **123**, 305 (1982).
[27] N. N. Avgul and A. V. Kieslev, in *Chemistry and Physics of Carbon*, edited by P. L. Walker (Marcel Dekker, New York, 1970), Vol. 6.
[28] J. Neugebauer and M. Scheffler, Phys. Rev. B **46**, 16067 (1992).
[29] F. Sim, A. S. Amant, I. Papai, and D. R. Salahub, J. Am. Chem. Soc. **114**, 4391 (1992).
[30] Y. Marcus, Chem. Rev. (Washington, D.C.) **88**, 1475 (1988).
[31] I. Bako, J. Hutter, and G. Palinkas, J. Chem. Phys. **117**, 9838 (2002).